ELSEVIER

Polymer 43 (2002) 4627–4638

polymer

www.elsevier.com/locate/polymer

Sol–gel derived composites from poly(silicic acid) and 2-hydroxyethylmethacrylate: thermal, physical and morphological properties

J. Habsuda[a,*], G.P. Simon[a], Y.B. Cheng[a], D.G. Hewitt[b], D.R. Diggins[c], H. Toh[c], Ferenc Cser[d]

[a]*Department of Physics and Materials Engineering, Monash University, Clayton, Vic. 3800, Australia*
[b]*School of Chemistry, Monash University, Clayton, Vic. 3800, Australia*
[c]*SOLA International Holdings Ltd, 19 Cooroora Crescent, Lonsdale, SA 5160, Australia*
[d]*Rheology and Materials Processing Centre, Department of Chemical and Metallurgical Engineering, RMIT, Melbourne, Vic. 3001, Australia*

Received 17 October 2001; received in revised form 7 February 2002; accepted 5 April 2002

Abstract

Hybrid materials based on poly(silicic acid) and 2-hydroxyethylmethacrylate were prepared and characterized. The glass transition temperatures of a homologous series of samples were measured by dynamic mechanical thermal analysis and the location of the transition and shape of the spectra shown to be dependent on the morphology of the inorganic phase which was able to be manipulated by variation of synthetic conditions. A number of other techniques including small angle X-ray scattering, electron microscopy, density and free volume measurements were used to help elucidate inorganic–organic miscibility and structure.

It was shown that incorporation of organic polymeric phase to crosslinked inorganic silicate led to the formation of the system that is similar to interpenetrating polymeric networks. A high level of miscibility as determined by small angle X-ray scattering and transmission electron microscopy was demonstrated. This was also demonstrated in DMTA traces as seen by the mobility of the organic phase being determined by the degree of crosslinking of the inorganic component. Nonetheless, there appear to be a slight influence of silicate architecture on molecular packing and miscibility. Highly branched, higher molecular weight silicate materials appear to be slightly less miscible.

Keywords: Composites; Small angle X-ray scattering; Positron annihilation lifetime spectroscopy

1. Introduction

ORMOSILs (ORMOCERs or CERAMERs) are materials which have been at the centre of attention of researchers involved in making organic–inorganic composite materials by applying principles of sol–gel chemistry for the last few decades [1–4]. The general character of the sol–gel reaction scheme, a condensation polymerization reaction, allows the incorporation of suitable polymeric/oligomeric components into the sol–gel network if such polymers or oligomers have appropriate functional groups [5] Therefore, the sol–gel process provides the opportunity to synthesize organic–inorganic nanocomposites or microcomposites that are impossible to prepare by traditional, high temperature processes due to the decomposition of organics [6].

Under appropriate conditions, the polymer remains homogeneously embedded within the inorganic gel throughout the synthesis and drying steps. A chemical bond (covalent linkage) between phases should thus be able to be established [7–15]. A number of polymers can, however, be dispersed within the system without formation of covalent bonds and if the components mutually penetrate, homogeneous and optically clear final materials can result due to the affinity for inorganic oxides through interactions such as hydrogen bonding [16–21].

In the present study, a synthetic approach towards organic–inorganic hybrid material based on pre-polymerization of poly(silicic acids) (PSA) was chosen. Molecular weights and molecular architecture of PSA were determined by means of gel permeation chromatography (GPC) and ^{29}Si nuclear magnetic resonance (NMR) spectroscopy. The properties of the products were influenced by the acid concentrations used and both the hydrolysis and condensation reaction times. The organic component was derived from 2-hydroxyethylmethacrylate (HEMA), which showed a good level of compatibility with the chemically dissimilar inorganic phase as a result of their mutual hydrophilic hydroxyl groups. However, contrary to previous published

* Corresponding author.

0032-3861/02/$ - see front matter
PII: S0032-3861(02)00246-X

reports and after much investigation, we have recently shown that no covalent coupling of the two phases could be established [22] in this type of sol–gel material. The major advantages of this two-step approach to sol–gel formation are the mild reaction conditions required, as well as the lack of a need to eliminate by-products such as alcohols, as in the traditional alkoxide sol–gel process, resulting in minimal shrinkage of the final product. Even though no chemical bond was formed between the two phases (PSA and HEMA) [22], high levels of association and mixing between organic molecules and the PSA component resulted in materials of good solid-state physical properties and a high degree of clarity, making them good candidate materials to coat and protect readily abraded plastics.

The use of chemical reaction conditions to vary the structure, morphology and miscibility of the inorganic phase within the polymeric matrix is likely to profoundly influence the resultant thermal, morphological and physical properties, and it is these which are reported in this paper.

2. Experimental work

2.1. Materials

Sodium metasilicate (97%) was purchased from Fluka, benzoyl peroxide from Ajax, 2-hydroxyethylmethacrylate (97%) and ethylene glycol dimethacrylate (98% pure) from Aldrich, hydrochloric acid, sodium chloride, sodium sulphate and tetrahydrofuran from Merck. Tetrahydrofuran was dried over lithium aluminium hydride, distilled from it and stored over sodium wire. It was subsequently distilled from sodium and benzophenone prior use. All other chemicals were used as received.

2.2. Synthesis of hybrid material

The target material was prepared using poly(silicic acid) (PSA) and 2-hydroxyethylmethacryalate (HEMA). Preparation of PSA involves hydrolysis and condensation of sodium metasilicate under acidic conditions. Hydrochloric acid concentrations of 3.0–6.0 M were used with reaction times of 1, 24, 48 and 72 h, respectively. It has been reported previously [22] that hydrochloric acid concentration used for hydrolysis of sodium metasilicate influences the degree of branching (Q values) in poly(silicic acids). ^{29}Si NMR spectra were used for determination of the Q values by integration of the peaks after subtracting the residual resonance from the glass tube (at δ −110 ppm). Q^4 peaks corresponding to fully substituted silicon with no OH groups attached were observed at δ −110 ppm, Q^3 peaks at δ −100 ppm and Q^2 at δ −90 ppm (see Ref. [22] for a precise structural assignment of these peaks). In these samples the ^{29}Si NMR spectra of acids produced under different reaction conditions clearly showed peaks corresponding to Q^2, Q^3 and Q^4. The Q^1 species, comprised less than 0.1% of the whole range of samples and was not affected by the changes in the reaction time or concentration of HCl. With increasing concentration of acid (3.0–6.0 M) and increasing reaction time (1–72 h), Q^2 values decrease in favour of Q^3 and Q^4 values, that is more branched and crosslinked species are formed. Molecular weights of the products vary slightly with the concentration of hydrochloric acid. In each set of the reaction times (1, 24, 48 and 72 h) molecular weights of the products increased as the HCl concentration increased, reaching values as high as 13 100. Molecular weights of the products produced with the prolonged reaction times up to 72 h produced species of similar molecular weights as high as 14 500.

In the subsequent synthetic step, HEMA was added to the PSA/THF solution, followed by an azeotropic distillation of water by THF at 64 °C. Following this, solvent was completely removed from the reaction mixture under reduced pressure (as monitored by ^{1}H and ^{13}C NMR spectroscopy) leaving a low viscosity colourless liquid.

The composite material was prepared by benzoyl peroxide initiated polymerization of the system in the presence of ethylene glycol dimethacrylate as a crosslinking agent. Samples were cured at 80 °C and postcured at 90 °C in a Teflon mould. The hybrid materials of different thickness obtained were transparent and colourless or slightly yellow.

2.3. Characterization techniques

Silicon nuclear magnetic resonance (^{29}Si NMR) spectra were recorded at 59.6 MHz with a Bruker AM-300 spectrometer using a standard 10 mm broad-band probe. The lock solvent was deuterated chloroform with TMS as an internal reference. Spectra were obtained using an average of 1000 scans per sample with a pulse width of 10 μs and a relaxation delay of 1 s. The ^{29}Si NMR spectra refer to tetrahydrofuran solutions of poly(silicic acids). Chromium(III) acetylacetonate ($Cr(acac)_3$, 0.1 M) was added as a non-polar paramagnetic relaxation agent in order to relax ^{29}Si through the unpaired electron spin density of the metal ion, and thus, to allow the time for data acquisition be shorter and also eliminate the NOE effect. Q values for poly(silicic acids) were determined by integration after subtracting the residual resonance from the glass tube.

Gel permeation chromatography (GPC) was performed on a Waters GPC system (Waters 6000A solvent delivery pump, Waters U6K injector and WatersR-401 detector). Columns were packed with Plgel Mix B 10u Linear (7.5 mm × 60 cm) and μstyragel 100 Å (7.8 mm × 30 cm). The samples were run at 1 ml/min with tetrahydrofuran as the eluant. Monodisperse polystyrene standards were used for molecular weight calibration. The products (poly(silicic acids)) are, of course, not linear and the GPC molecular weights are unlikely to be precise. The hydrodynamic volume of highly branched polymers is less than in the linear polymers of equivalent molecular weights. Thus, molecular weights determined by GPC are underestimated

compared to the real values of the branched systems of poly(silicic acids). However, they should provide a reasonable estimate of relative molecular size.

Dynamic mechanical thermal analysis (DMTA) was performed on a Perkin Elmer DMA 7 (penetration probe mode). Samples of 18 mm × 4 mm × 2 mm (width × depth × height) were tested in the temperature range of −130 to 150 °C, at a heating rate of 2 °C/min and 1 Hz frequency. The sample chamber was purged with helium during the run. Pure indium and *n*-octane were used for calibration over a wide temperature range.

Differential scanning calorimetry (DSC) was undertaken using a Perkin Elmer DSC 7. Samples were run in the temperature range between 30 and 180 °C under nitrogen at a scanning rate of 10 °C/min followed by quenching, and rerun in the same temperature range at 20 °C/min. The instrument was calibrated with indium and zinc.

Small angle X-ray scattering (SAXS) measurements were performed on a Rigaku SAXS System with a Kratky camera. The wavelength of the Cu Kα X-ray was 1.5419 Å. The Rigaku X-ray generator was utilized. The operational voltage was 30 kV with a current of 30 mA. Continuous data collection in a scattering angle range of −1 to +1 degree, 2θ with steps of 0.002° at scattering rate 0.04 deg/min was performed at ambient temperature. Background collection was performed under the same conditions as the sample data collection prior the data collection. The background counts were scaled and removed from the scattering beam.

For the transmission electron microscopy (TEM) studies, a bulk specimen of each sample was cut to a size 2 mm × 7 mm × 1 mm and put in the cryochamber of the Reichert Ultracut FCS. Ultrathin sections were cryomicrotomed using a diamond knife at −30 °C, adjusted by ±10 °C depending on the sample behaviour. The sections were transferred to copper grids of 300 or 400 Å mesh. The sections were imaged on a Phillips EM 420 at 80 and 100 kV, respectively.

One of the more novel characterization techniques used in this work was positron annihilation lifetime spectroscopy (PALS). This is a radioactive technique which uses the injection of sub-atomic particles, positrons (the antiparticle of electrons), into the sample to determine the angstrom-sized, free volume pores in materials. It has been increasingly widely applied in polymer physics and the details of the subatomic processes and experimental conditions and applications of it to polymers have been well detailed elsewhere [23–25]. It has been found that the excluded volume is relevant to properties such as gas and moisture permeability, ageing, temperature effects such as the glass transition and to mechanical deformation [26]. Whilst the positron itself decays and forms various species, it is the lifetime of one of these, *ortho*-positronium (*o*-Ps) that has been found to best correlate with free volume in polymers. The lifetime τ_3 and its intensity, I_3, are related to size (radius) and concentration of free volume holes, respectively. Use of an empirical equation and various assumptions about hole shape allows an estimation of the hole radius, r, and its volume, $V(=(4/3)\pi r^3)$. A measure of the total free volume is given by multiplying V by I_3. To date, PALS results have not been reported for ORMOSIL/CERAMER systems, although there have been some reports for non-organic-based sol–gels [27–29].

The PALS measurements were made using an automated EG&G Ortec fast-fast coincidence system with a ^{22}Na resolution of 270 ps. The equipment was thermally stabilized at 22 ± 0.5 °C to reduce electronic drift. The ^{22}Na positron source of approximately 30 μCi activity consisted of a 2 mm diameter spot source of 1.3 MBq sandwiched between two 2.5 μm titanium foil sheets. It was found that there was no significant source contribution based on single lifetime (166 ps) spectra for 99.99% pure annealed and chemically polished aluminium samples. The source-sample geometry consisted of the source sandwiched between two identical composite samples and whole source-sample assembly was sandwiched between the two detectors. All data were collected at 22 °C with 10 spectra of 30 000 peak counts being collected for each sample. Error bars are population standard deviations of these results. The PALS spectra were modelled as the sum of three decaying exponentials using the PFPOSFIT program. The short lifetime was fixed at 0.125 ns characteristic of *p*-Ps annihilation in molecular solids.

As a comparison with free volume, bulk density was measured using a Micromeritics AccuPyc 1330 Helium Pycnometer. The device works by using the pressure of helium to accurately determine the volume of a sample of known mass and thus requires no immersion in solvents.

3. Results and discussion

3.1. Thermal behaviour

On the basis of the NMR, FTIR, GPC and HPLC studies we earlier reported [22] that there is *no* chemical bond in the system based on poly(silicic acid) produced by acidic hydrolysis of sodium metasilicate and HEMA, and that both co-exist as independent polymeric networks [22]. However, as outlined below, it is clear that the reaction conditions (those to pre-form the PSA) and the resultant morphology remain strongly interrelated.

Measurement of glass transition temperatures of the composites was attempted using DSC. The determination of the glass transition of some polymers by DSC can be difficult as it involves a relatively small step change in heat capacity, especially compared with other major thermal transitions such as melting and crystallization. Samples of the composite materials and PHEMA were run on the DSC after being stored at ambient temperature, and exposed and equilibrated in the moisture in the air. In addition, some composite samples (reaction conditions for PSA

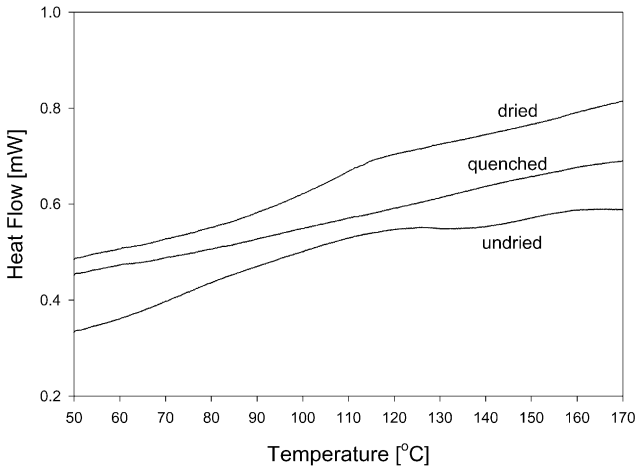

Fig. 1. DSC scans of PHEMA.

preparation: HCl concentration of 4.0 and 5.0 M, both with a 1 h reaction time) were dried at 80 °C for 8 h and kept in desiccator prior to measurement. For comparison, polymeric HEMA (undried and dried) was produced and measured and showed a glass transition at ~110 °C (Fig. 1). Note that the heat flow scale (related to heat capacity) is very small. Following this run, the PHEMA sample was quenched and run again, with no glass transition observed during this second heating run. DSC scans of dried composite samples (Fig. 2(a)) and quenched samples (Fig. 2(b)) exhibited no observable transitions and were almost identical in appearance. Undried composite samples showed a very broad transition over the whole heating temperature range (Fig. 2(c)). The fact that the transitions of the composite materials were less sharp and not similar to that of the PHEMA polymer indicated that the polymeric phase might be mixed to some degree with the inorganic phase, resulting in a range of diverse molecular environments which broaden out the glass transition region. The glass transition appeared to be a little stronger and more obvious in undried samples (Fig. 2(c)) compared with the dried ones (Fig. 2(a)). The presence of moisture in the undried samples also led to broader transitions than for the dried samples (Fig. 2(c)). This is probably due to microheterogeneous distribution of water molecules in the matrix and the range of molecular environments in which the polymer chains find themselves.

The DSC scans were thus not successful to any real degree in determining T_g, given their largely featureless nature. Given that the glass transitions observed were broader and different in appearance from those of pure PHEMA, it was suggested that the composite system is composed of a fine dispersion of an inorganic phase within the organic matrix and as a result of mixing at some level, the T_gs of the final systems were affected and their strength reduced. Importantly, however, DSC scans clearly showed that there was no reacting exotherm peak, suggesting that the system (HEMA and EDGMA) is fully thermally cured.

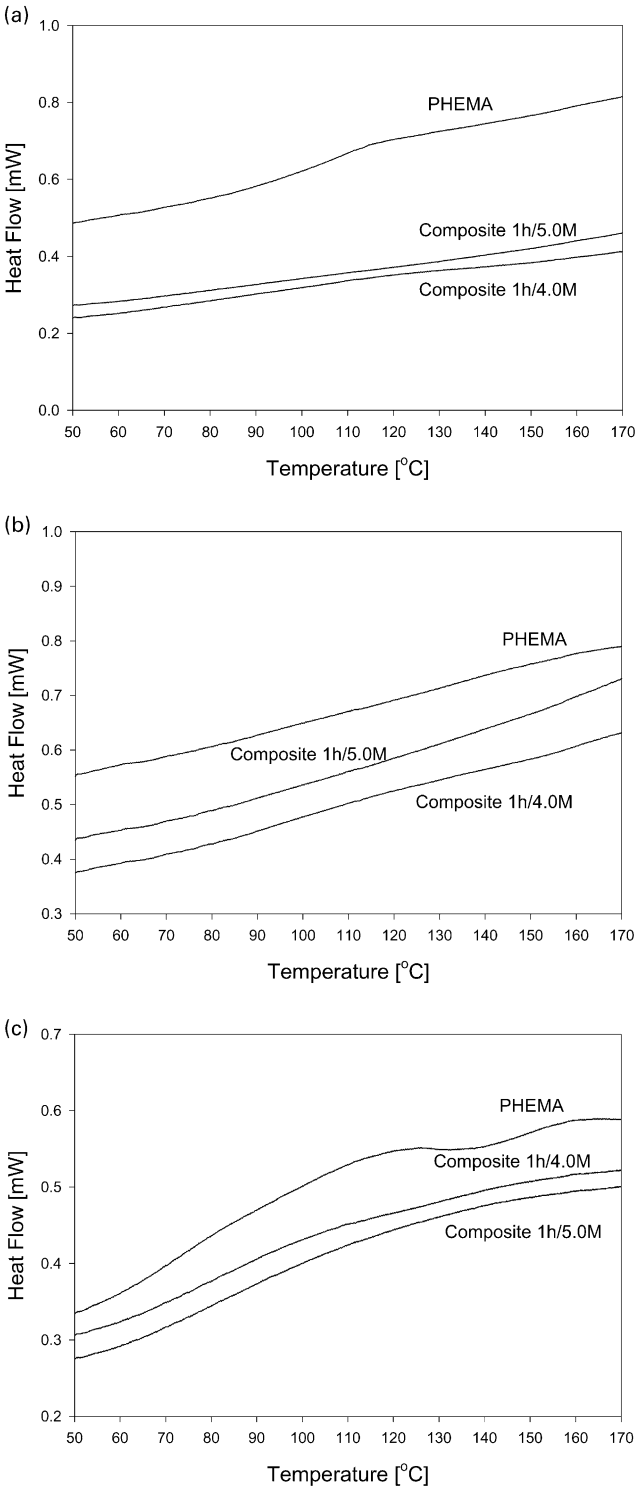

Fig. 2. (a) DSC scans of dried samples of PHEMA and composites (1 h/4.0 M and 1 h/5.0 M). (b) DSC scans of quenched samples of PHEMA and composites (1 h/4.0 M and 1 h/5.0 M). (c) DSC scans of undried samples of PHEMA and composites (1 h/4.0 M and 1 h/5.0 M).

It should be noted that even though the samples were dried at temperatures 30 °C below T_g, there did not appear to be evidence of thermal ageing in the polymeric HEMA or the PHEMA-phase of the composites. This would normally be

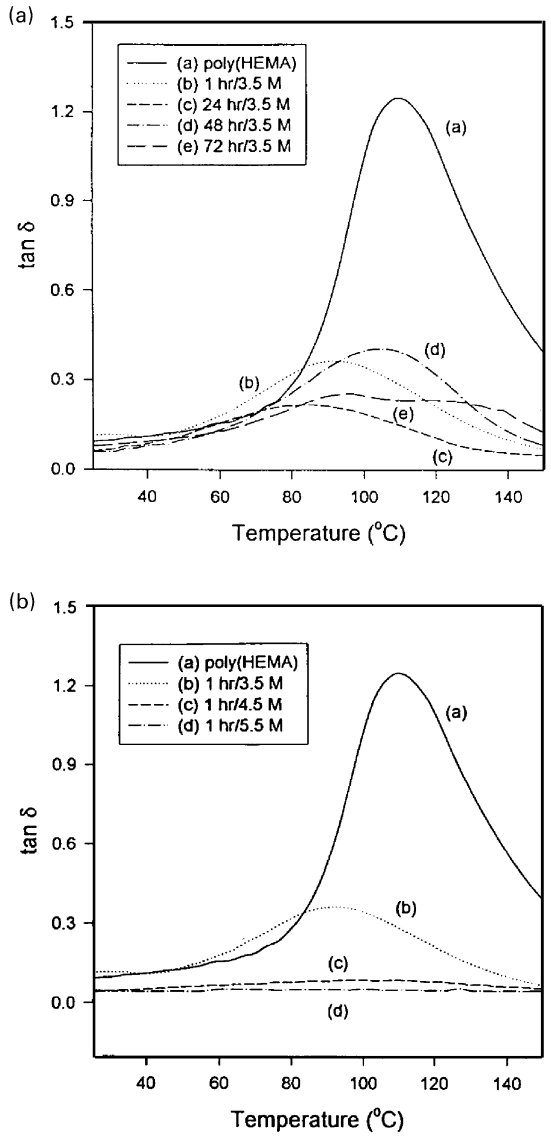

Fig. 3. (a) tan δ vs temperature of PHEMA and composites at variable reaction time. (b) tan δ vs temperature of PHEMA and composites at variable c_{HCl}.

observed as an overshoot in the heat capacity curve (enthalpy recovery) and could in fact increase the possibility of observing a (albeit modified) glass transition temperature.

However, the T_g of PHEMA and the composites was able to be determined using the DMTA technique and results of tan δ against temperature are shown in Fig. 3 for a number of systems. Details of the spectra such as the location of the maxima of tan δ peaks, width at half height ($W_{1/2}$) of peaks and the presence and location of any secondary relaxations observed below the glass transition are presented in Table 1. PHEMA was found to show a readily observed glass transition relaxation at ~110 °C. It can also be seen that the shapes and positions of the α-relaxations of the composites are quite different from the PHEMA and each other, and are strongly dependent on the reaction conditions of the PSA component and thus presumably to the overall degree of mixing and morphology in the final composite. The width of the DMTA peaks for the majority of the composites was broader than those for PHEMA. Broadness of the tan δ peaks and a measure of the relaxation strength (the height of the tan δ peak) varied as a function of different reaction conditions which produced different morphologies. Even though integrated area under a loss peak is more strictly a measure of the strength of a relaxation peak [30], the height of the relaxation peak also remains a ready and useful means of comparison.

Although the T_gs of the composite systems changed with changes of HCl concentration and reaction time, there is no clear correlation between glass transition temperatures and these two primary parameters. It is thus likely that the dynamic mechanical behaviour in composite samples could be due to a number of factors, resulting from different reaction conditions and formation of a variety of branched silicates. In a broader sense, changes in glass transition temperatures of the composites appear to correlate with the structure of the poly(silicic acids) (Q values) and molecular weight (M_w) of the inorganic component in the composites. A higher Q^3 content (and thus less branched structure) could be expected to lead to better molecular interactions and miscibility, resulting in greater chain constraint and thus, higher glass transition values, and this was observed. The T_g of the PHEMA phase decreased with increased Q^4 values indicating a more highly branched inorganic network less likely to be miscible with the lightly crosslinked organic phase. Since the sum of Q^3 and Q^4 tend to be relatively constant overall, it can be concluded that an increase in Q^3 leads to better organic–inorganic molecular mixing, better subsequent chain packing and higher T_g. The general decrease in T_g with changes in molecular weights is explainable in similar miscibility terms—increasing PSA molecular weight to lead to poorer mixing of PHEMA and PSA components due to a lower entropy of mixing. A lower molecular weight PSA (for a given degree of branching) could be expected to be more miscible—with a greater resultant T_g.

In addition to the observation that the glass transition temperature varied from sample to sample as a result of different structural features of the inorganic phase, a strong variation in the broadness of the peaks was also observed. It was found that the majority of tan δ peaks of the composites were broader than that of PHEMA, with more significant changes in broadness occurring as a result of differences in HCl concentration of PSA synthesis, compared with the effect of polymerization time on the incorporated inorganic component. Generally, it appears that for PSA materials produced at higher concentrations of HCl, the DMTA relaxation broadness increases. Composites containing PSA phases which are more highly branched (higher Q^4 values) which result from higher acid concentrations during PSA synthesis (3.5 and 4.0 M composites) show broader tan δ peaks. The reduction in broadness with decreasing Q^4 (increasing Q^3) is surprising in the sense that, as

Table 1
Dynamic Mechanical glass transition temperatures (T_g) and secondary relaxation data of PHEMA and some of the composites determined from tan δ plots

Reaction time (h)	c_{HCl} (M)	T_g[a] (°C)	$W_{1/2}$[b] (°C)	Secondary relaxation (°C)	Relaxation strength[c]	Q_4 (%)
PHEMA	–	111	42	− 87	1.30	–
1	3.0	128	40	− 71	0.55	25
	3.5	93	57	− 79	0.36	38
	5.5	80	92	− 85	0.06	35
	6.0	123 (67)	109	− 86	0.12	33
24	3.0	122	45	− 79	0.73	34
	3.5	84	56	− 79	0.22	45
	5.5	111	62	− 72	0.26	59
	6.0	99	100	− 72	0.13	69
48	3.0	121	47	− 70	0.42	43
	3.5	104	58	− 76	0.40	52
72	3.0	141 (107)	35	− 72	0.6	33
	3.5	99 (125)	60	− 75	0.25	55

[a] Values in parantheses show the 'shoulders' of α-relaxations.
[b] Width of the peak at half height.
[c] Determined by taking the height of tan δ peak.

proposed previously, less branching would be thought to lead to miscibility. Broadness in glass relaxation temperature regions is well known to increase in conventional, miscible thermoplastic blends due to microconcentration fluctuations [31–33]. Thus, the broader relaxations observed with less miscible, more highly branched PSA (higher Q^4) cannot be simply assigned to effects of miscibility. In this case, broadness of higher Q^4 materials may be due to a more dispersed, defined structure of the branched material causing a wide range of molecular constraints and thus a greater variety of regions of molecular motion. This would be due, in part, to entanglements at the interface and/or constraint of polymers between inorganic regions [31].

This is really analogous to the idea of many different constrained polymer regions around the branched PSA. However, unlike conventional inorganic fillers, the nanosize of the silicate region means the effect is much stronger. Indeed, as can be seen in Fig. 3, the strength of the relaxation peaks for all composites is less than that of the polymer due to the presence of the inorganic phase. In a quantitative sense, relaxation strength defined by the heights of tan δ peaks correlated well with the degree of branching and molecular weights of the inorganic PSA network. With increased level of immiscibility (due to higher Q^4 and M_w values of the PSA component) the magnitude of the peak height due to the organic PHEMA phase appears to be suppressed due to reduced chain mobility. It may be expected that there would be a reduction in relaxation strength due to a dilution effect. However, even though the inorganic phase content is relatively small (up to ~10 wt%) compared with the organic component, a very significant decrease in relaxation strength occurs.

Such a reduction of tan δ peaks of the composites compared with that of the polymer due to the entrapment of the polymer chains within an inorganic network has been reported previously for composites such as PMMA/SiO_2 and PVAc/SiO_2 with inorganic phase content of approximately 24 wt% [18] as well as for PDMS/Al, Ti or Ta based composites [34]. As with the discussion of broadness, it is likely that it is the very fine scale (and thus high surface) of the inorganic phase that leads to such a strong reduction of relaxation strength. It should also be noted that the presence of a crosslinking agent such as EGDMA in the composite system might reduce relaxation strength slightly as it causes reduction of the polymer chain mobility compared with pure PHEMA. However, the concentration of crosslinker used in the present study is small (2%) and would not be expected to have such a significant effect on relaxation strength.

Secondary relaxations or sub-T_g relaxations are due to local motions of the polymer chain (main or side) and functional groups. They are usually smaller in magnitude than the primary relaxations and follow an Arrhenius-type relationship when log of the frequency maxima is plotted as a function of reciprocal absolute temperature. They reflect the nature of the glassy state of the polymer matrix. It has been shown recently in many systems, for example in polyacrylates [35] and side chain liquid crystalline polymers [36], that even though they often represent very local motions, they are still reflective of the properties of the glassy state (packing, orientation and even molecular weight).

A secondary relaxation occurs in PHEMA due to the localized motion of the polar side chains at around −87 °C, as determined from tan δ peak. In the composite samples, this location varied as a function of acid concentration in the synthesis of the inorganic phase and may be indicative of changes in the glassy environment in which the side chain resided. Location of secondary relaxation peaks for all samples appeared to be at higher temperatures than for the neat polymer. In our systems, the local motion of the

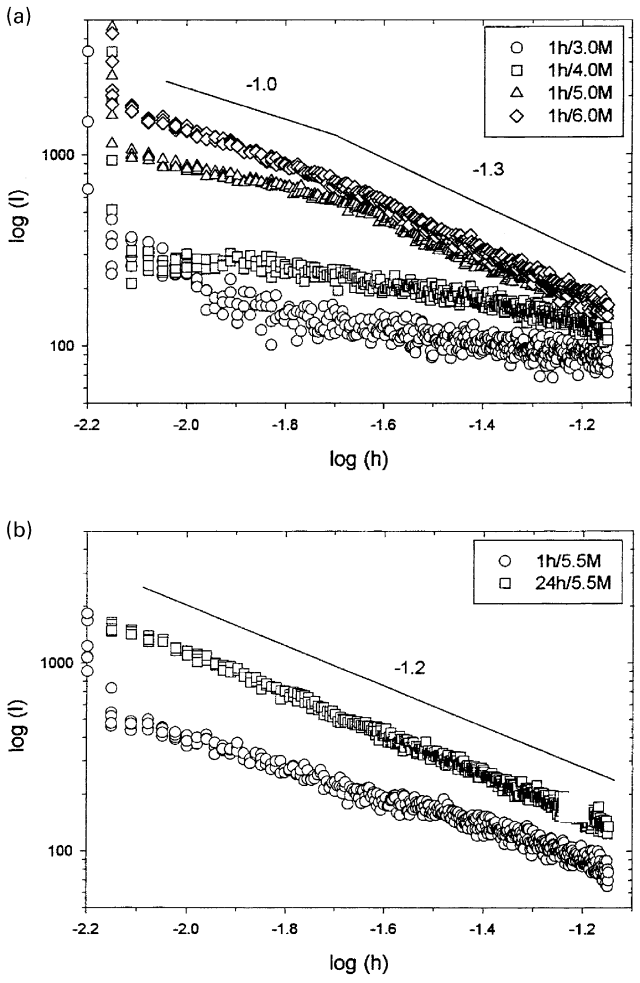

Fig. 4. (a) Double logarithmic plots of SAXS intensities for samples prepared at 1 h and variable c_{HCl}. (b) Double logarithmic plots of SAXS intensities for samples prepared at c_{HCl} 5.5 M and variable polymerization time.

side group is affected greatly by the glassy environment. Although clear trends are hard to find, the fact that the values of the secondary relaxation temperatures are higher than for neat PHEMA could be an indication that there is some level of molecular mixing or constraint between the polymeric and the inorganic components. It was argued above that the glass transition might be affected by becoming confined between regions of discrete inorganic phases (in addition to mixing with inorganic material in a miscible fashion). The fact that a more local motion than the α-relaxations is also affected, suggests that such constraints could be quite strong.

3.2. Morphology of the system

The SAXS technique allows the structure of the scattering sample to be determined using the intensity of the scattered X-ray beam and the dependence of this intensity on the scattering angle, θ [37]. Some knowledge or assumed model structure is normally required to aid interpretation of the SAXS data. In this work, the concept of *fractal geometry* for determination of morphology has been employed [38]. Even though the materials of the present study are amorphous, there are fluctuations in electron density due to the chemical differences between inorganic and organic segments and information about the morphology of the system may be obtained.

A double logarithmic plot of SAXS intensity (I) versus scattering vector (h), where $h = 4\pi\ sin(\theta)/\lambda$, 2θ is the scattering angle and λ is the wavelength of the beam, was produced for each composite sample and power law values were obtained as the slopes of the plots ($\partial \log I/\partial \log h$). All samples in which the inorganic phase was produced using variable HCl concentration and reaction time produced scattering as a result of the presence of environments with different electron densities, inorganic SiO_2-rich electron densities and lower electron densities of the polymer matrix. Scattering intensities and power law behaviour vary, despite the fact that the inorganic phase content is quite low and does not change significantly (maximum of 10 wt%) within the range of samples (Fig. 4). It is clear that the morphologies differ, and are dependent on the reaction conditions used for the hydrolysis and condensation of sodium metasilicate to form the incorporated poly(silicic acid).

The SAXS intensity, which reflects the relative electron density difference between phases, varied within the range of composite samples, suggesting that there are some differences in the phase behaviour (miscibility) in the samples made under different reaction conditions (HCl concentration, reaction time). It can be seen that the scattering intensity increases as the c_{HCl} increases for samples made at 1 h reaction time at all angles (Fig. 4(a)). It also appears that the reaction time of the metasilicate hydrolysis and condensation also affect the scattering intensities of the samples. For example, for 5.5 M, the intensity was higher with prolonged reaction time (Fig. 4(b)). Even though the scattering intensities for each sample were quite low, the increasing trend with time suggests a slight increase in immiscibility of the phases within the composite systems due to the structural changes (Q^3, Q^4 values and M_w in Table 2). As it has been discussed previously [22], with increasing PSA values of Q^4 and molecular weights there is less miscibility in the system and a greater phase separation resulting in higher scattering intensity. Conversely, with increasing Q^3 concentrations and molecular weights in PSA, degree of mixing between phases is greater with inorganic network more finely dispersed throughout the organic matrix, allowing more interactions resulting in lower scattering intensity.

Overall, it can be seen that the maximum power law of all the samples reported here was of −1.8 (48 h/4.0 M). This is still quite low compared with other sol–gel systems reported previously in the literature [39,40]. The scattering intensities of the range of the composite systems are indicative of the degree of phase mixing and an indication of the size/shape of the phases within the overall morphology. Higher values (near −3 or −4) [39,40] indicate that the differences

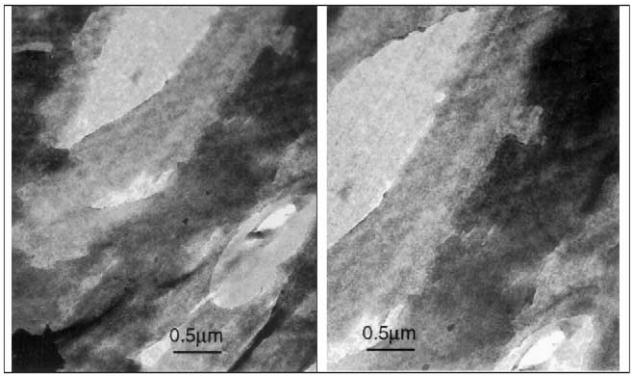

Fig. 5. TEM micrograph of a 1 h/6.0 M composite.

in electron density between phases are larger and thus the presence of well-defined, sharp three-dimensional structural features are present within the composite morphology. For systems with lower values of power law exponents the difference in densities of both phases is less, and the possibility of finer morphology more likely and this is observed in our work. For power law values of zero, mixtures are miscible at some level, with no distinct phases present.

In the present systems the low scattering and low power law values (−1) may suggest no definite phase separation with the inorganic phase finely dispersed throughout organic matrix. Thus, the system based on PSA and polymer is a partially miscible system with no distinct phase separation and clear boundaries between both phases. It appears that inorganic phase can interact with the organic network due to its structural features with, as mentioned before, higher Q^3 concentrations producing a more wispy type of morphology allowing mutual interactions and interpretation between components. This appears to be quite different from sol–gels previously reported (prepared from tetraethyl orthosilicate and 2-hydroxyethylacrylate) where well-separated, sharp and distinct globules with higher power law exponents (−3, −4) [40] were observed.

Transmission electron microscopy (TEM) provides detailed structural information at levels down to nanometer dimensions. The majority of sol–gels are optically transparent but generally show a pattern in a submicrometer range. The contrast between phases in the TEM is attributed to density differences between the organic polymer and SiO_2-rich phases. In the images, the white phase represents organic polymers, while more electron-dense silicate phase appears dark. However, any contrast observed might also originate from differences in mass thickness, as has been shown before in studies of amorphous blends and care must be taken in the analysis of such samples [39].

Previously, micrographs of organic–inorganic hybrid systems have been presented [39–42] and the morphology observed was dependent on the nature of polymerization, sequential or simultaneous. Systems showed quite uniform morphologies with more distinct contrast in TEMs of samples polymerized sequentially. Morphology of the

Table 2
Power law values of the composite samples from small angle X-ray scattering data

Reaction time (h)	c_{HCl} (M)	Power law	Q_3 (%)	Q_4 (%)	M_w
1	3.0	− 0.4, −1.4	59	25	5429
	4.0	− 0.3	43	47	9384
	5.0	− 1.3, −0.5	52	38	15 352
	6.0	− 1.3, −1.0	61	33	24 907
24	3.0	− 0.7	52	34	8811
	4.0	Unspecified[a]	45	47	16 528
	5.0	− 1.2	46	46	–[b]
	6.0	− 1.0, −1.6	30	69	–[b]
48	3.0	Unspecified[a]	47	43	10 032
	4.0	− 1.0, −1.8	40	49	13 592
72	3.0	− 1.1	57	33	21 388
	3.5	− 1.0	37	55	29 831

[a] No definite pattern was observed in the samples possibly due to very low scattering intensities with attendant high experimental error.
[b] Molecular weights of 24 h/5.0 and 6.0 M samples could not be determined as the samples caused blockage of the GPC columns.

samples synthesized simultaneously was more difficult to determine because, although a texture was apparent, the size scale was difficult to specify as the interfaces appeared to be quite diffuse. Silica within the system was apparent as the second phase. It has also been reported [42] that the presence of a catalyst (base or acid) influences the mechanism of the sol–gel reaction and the morphology of the systems. The base-catalysed system showed silica rich domains (0.1–0.2 μm) that tended to form clusters (1–5 μm in diameter). On the other hand, the acid-catalysed morphology was very uniform and domains could not be observed even at high magnifications and particles were possibly too small to be resolved (probably smaller than 100 Å).

Composite materials produced in this work were viewed using TEM and found to be optically transparent and the samples appeared to be susceptible to degradation by the electron beam. The intensity of the beam had to be adjusted carefully to minimise decomposition of the thin sections. The TEM images showed contrast in colour and patterns. However, it seems that any patterns or contrasting of regions were due to the sectioning pattern, rather than the presence of a dark inorganic and light organic phase. The best images obtained in this work were taken from the sample 1 h/6.0 M (Fig. 5) which allowed tentative assignment of the fractal pattern observed by SAXS. The contrast (dark and light regions) is sufficient to see two phases which are quite diffuse, with no clear boundaries. This is indicative of the presence of islands of inorganic phase. The very fine morphology observed in the 1 h/6.0 M sample appears to have an approximate domain size of the order of 20–50 nm. The lack of any features in the TEM images appeared to be a result of very fine morphologies formed from the PSA produced from the starting material in the

Table 3
Densities of poly(silicic acids) and PHEMA

Reaction time (h)	c_{HCl}, poly(silicic) acids (M)	Density (g/cm^3)
1	3.0	1.7592 ± 0.0012
	3.5	1.9886 ± 0.0122
	6.0	1.6293 ± 0.0013
72	3.5	1.9312 ± 0.0082
PHEMA		1.2730 ± 0.0003

presence of an acid as a catalyst, and polymerized organic network. It has been shown [39–42] that much finer morphologies showing a very limited number of features in the images are produced in acid-catalysed system compared to base-catalysed. Overall, this implies that the PSA is well dispersed and miscible with the organic network causing low scattering intensities and power law values by SAXS as shown in our work. Indeed, the composites based on TEOS and HEA [40] of higher SAX intensities and higher power law values (−3, −4) produced strong TEM images with distinguished features with the inorganic domain size of 600–900 Å.

3.3. Physical properties

The measurement of physical properties such as density and free volume was also used to determine the influence of the phase co-existence, and thus the degree of packing, on the properties of the resulting materials. The densities of the PHEMA, poly(silicic acids) and composite materials were measured using the gas pycnometer and are summarized in Tables 3 and 4. The composite samples consist of an inorganic phase (poly(silicic acid)) and an organic phase (PHEMA). The density values of PSA and HEMA can thus be taken as the limiting values. It was expected that the values for the composites would be within the range of PSA and PHEMA densities and dependent on composition. As the silica content (determined by TGA) was less than 10 wt% for most samples in Table 4, polymer was the major component and the density values were expected to be closer to that of PHEMA than PSA, and this was confirmed by experiment. The density values of all composites were in the range 1.28–1.32 g/cm^3 and thus close to that of PHEMA (1.27 g/cm^3).

Densities of the PSA appeared to be slightly below that of quartz, i.e. fully condensed SiO_2 (2.20 g/cm^3). The values for PSA 1 h/3.0 M (1.76 g/cm^3) and 3.5 M (1.99 g/cm^3) showed a positive trend with increasing concentration of acids. However, the experimental error for value of PSA 1 h/6.0 M (1.63 g/cm^3) may be quite high as the acidic sample damaged the surface of the measurement cell. The density of PSA 72 h/3.5 M was slightly lower than that of the 1 h/3.5 M sample. Interestingly, there was no clear trend in the densities of the composites as a function of silica content below 10 wt%. It might have been expected that density would increase largely based on the SiO_2 content. Such a clear trend was observed for samples with much higher silica contents, however, increasing from 10 to 33 wt% (Table 5).

Table 5 summarizes the calculated and measured densities of some of the composites. The values of density calculated were close to 'rule-of-mixtures' (additivity) calculated densities as shown in Table 5. This seems to indicate additive behaviour as would be expected if the phases are not fully intermixed (miscible) and the interfaces are good. If the interfaces were poor, extra volume at the interface could be expected to lead to lower densities than expected from additivity. Changes in densities as a function of SiO_2 content have been previously reported [41]. In that work silicate contents as low as ~14 wt%, yielded densities close to that of the neat polymer. The density of the composite samples of ~90 wt% silicate were reported to be as high as ~1.8 g/cm^3 [41]. It has also been reported [43] that although density increases with the SiO_2 content, it is also often dependent on the structural features resulting from the variable degree of interactions between organic and inorganic phases. Greater interactions led to the systems with minimal

Table 4
Densities of the composite samples

Reaction time (h)	c_{HCl} (M)	SiO_2 content [TGA] (wt%)	Density (g/cm^3)
1	3.0	6.8	1.3134 ± 0.0014
	4.0	7.4	1.2878 ± 0.0008
	5.0	8.7	1.3197 ± 0.0008
	6.0	10.6	1.3063 ± 0.0007
24	3.0	7.1	1.3194 ± 0.0014
	4.0	8.7	1.3198 ± 0.0004
	5.0	9.3	1.3114 ± 0.0006
	6.0	4.9	1.2835 ± 0.0003
48	3.0	6.7	1.3009 ± 0.0003
	4.0	5.1	1.3020 ± 0.0007
72	3.0	7.5	1.3196 ± 0.0011
	3.5	7.7	1.3139 ± 0.0006

Table 5
Density of composites (based on PSA 1 h/3.5 M) as a function of SiO_2 content

Reaction time/c_{HCl} (h/M)	Molar ratio, PSA/HEMA	SiO_2 content [TGA] (%)	Measured density (g/cm$_3$)	Calculated density 'rule of mixtures' (g/cm^3)
1/3.5	1:6	7.2	1.3111 ± 0.0006	1.3178
	1:3	13.0	1.3341 ± 0.0009	1.3326
	1:1	33.0	1.5053 ± 0.0018	1.4405

volume at the interface resulted in higher densities than the rule-of-mixtures.

It is clear that interactions and packing is a key factor in the behaviour of those systems. The PALS technique was used in an attempt to probe such properties. As mentioned before, it has not been previously applied to CERAMER or ORMOSIL systems. In inorganic silica gels [29] it has been reported for materials where varying compositions of tetrasulphonic acid, tetramethyl orthosilicate and sodium hydroxide, water, methanol were combined. For the silica xerogel formed, it was found that four (rather than three) lifetimes fitted the data. An inverse relationship was found between free volume determined by this technique and bulk density.

Also relevant is the fact that the PALS technique has been widely used to understand the free volume of polymers in multicomponent mixtures such as polymer blends [23,44,45]. A number of samples were run in this work and fitted to the three-lifetime model. The two basic parameters, the lifetime τ_3 and the intensity I_3, were determined as well as the subsequently determined radius of fractional volume, r, volume of the free volume sites, V, and total free volume (estimated by multiplying V by I_3) and these parameters are summarized in Table 6. Unfortunately, the PALS data of poly(silicic acids) could not be measured as they were in the form of powders.

The values of τ_3 of the hybrid materials were found to be quite similar to that of PHEMA as expected since they were all around 85–95 wt% PHEMA. However, this means that any variations seen are likely to be due to influences of the PSA on the polymeric phase. There seems to be a slight variation in τ_3 (size) with acid concentration (at a given PSA polymerization time) with a slight increase for higher acid levels. The change in I_3 is not monotonic, but if anything it increases slightly with acid level. As a consequence, $V \times I_3$ (a measure of total free volume fraction) also seems to increase slightly with acid concentration, although this is not true in the 1 h polymerization set of materials. This is despite the bulk density of these samples (Table 4) showing no differences. The general trends observed (especially in 24 and 48 h samples) are consistent with higher acid concentrations leading to more branched PSA structures (higher Q^4) which are less miscible in the organic matrix, as seen in corresponding changes in the T_g of the PHEMA phase and scattering intensity, mentioned earlier. The increased free volume size and concentration could be due to free volume generated at the increasingly defined interface of these two materials which have been shown recently to be non-covalently joined [22]. It was found previously that in an immiscible thermoplastic blend system [44] there was a synergistic increase in free volume in immiscible blends (compared to just average behaviour) and this was attributed to poor interfaces generating larger free volume and the same factors could be at play in this system.

Furthermore, if acid concentration is fixed (3.0 M) but PSA polymerization time varied (and thus PSA molecular

Table 6
PALS data of PHEMA and some of the composites

Time (h)	c_{HCl} (M)	τ_3 (ns)	I_3 (%)	Free volume radius r (Å)	Volume V (Å^3)	Free volume fraction $V \times I_3$
PHEMA		1.73 ± 0.02	20.66 ± 0.40	2.59 ± 0.09	73.38 ± 3.80	1516.03
Quartz		1.57 ± 0.01	51.31 ± 0.82	2.42 ± 0.05	59.53 ± 1.80	3054.48
1	3.0	1.73 ± 0.02	20.74 ± 0.42	2.60 ± 0.09	73.38 ± 3.80	1521.90
	3.5	1.70 ± 0.01	20.59 ± 0.18	2.56 ± 0.04	70.49 ± 1.80	1451.39
	5.5	1.76 ± 0.02	18.21 ± 0.32	2.62 ± 0.08	75.62 ± 3.80	1377.04
	6.0	1.74 ± 0.02	17.57 ± 0.30	2.61 ± 0.09	74.12 ± 3.80	1302.29
24	3.0	1.66 ± 0.02	21.22 ± 0.33	2.52 ± 0.09	67.06 ± 3.70	1423.01
	5.0	1.73 ± 0.02	17.86 ± 0.33	2.59 ± 0.09	73.38 ± 3.80	1310.57
	6.0	1.85 ± 0.01	20.58 ± 0.27	2.71 ± 0.04	83.66 ± 1.90	1721.72
48	3.0	1.62 ± 0.01	20.82 ± 0.31	2.48 ± 0.05	63.80 ± 3.60	1328.32
	3.5	1.72 ± 0.02	20.86 ± 0.41	2.58 ± 0.04	71.92 ± 1.80	1500.25
72	3.0	1.69 ± 0.03	20.66 ± 0.48	2.55 ± 0.13	69.79 ± 5.60	1441.86

weight), a general decrease in τ_3 (free volume pore size) and a slight decrease in I_3 is also observed. Although this is true for the 1, 24 and 48 h samples, the value of τ_3 and I_3 increases again for the longest time of 72 h. As a result, there is an average decrease in total fractional free volume measured by PALS although, as before, density does not show such a clear trend. The scattering work mentioned above would indicate that greater immiscibility could be expected with higher molecular weight of PSA samples and thus, using the argument developed above for acid concentration effects, greater values of τ_3 and/or I_3 may have been expected. However, the reverse occurs and thus the simple model of miscibility/immiscibility and the prospect of additional free volume generated at interfaces may be too simple. Clearly, despite the fact that only low amounts of inorganic phase exist, they are very small and hence, due to a large surface area (the precise nature and topography of the surface of the silicate phase being difficult to conceptualize) interact with and influence much of the bulk organic phase. This may alter the packing of the organic phase, leading to broader and weaker dynamic mechanical relaxation peaks and also influence free volume and packing probed by PALS. Material constrained around nanoscale 'particles' would be expected to show tighter packing and thus lower values of τ_3 (pore size). It should be noted that the variation in τ_3 and I_3 with PSA polymerization time is not as great as for a system of a given PSA single polymerization time in which the acid concentration is varied.

4. Conclusions

This study of the PSA/HEMA composites reveals that materials with good mechanical properties and a high degree of clarity can be produced, even though there is no covalent bond between organic and inorganic phase. Although the organic phase dominates the overall composition, the properties of the materials appeared to be strongly affected by the presence of the inorganic phase, no doubt due to their very small nanosize.

Generally the glass transition temperatures of the range of the composites were similar to that of PHEMA as the composition of the materials produced is dominated by the polymer phase. The strength and breadth of relaxations did, however, vary strongly from sample to sample and a broad correlation was found with variables such as HCl concentration and reaction time, the greater degree of branching and molecular weight of the PSA phase produced, resulting in greater immiscibility, and seemingly more molecular constraint (broader relaxations).

The SAXS plots in this work revealed that the power law values and scattering intensities in all composite materials are quite low compared with those previously reported. Thus, it can be concluded that the sol–gel materials based on PSA and HEMA in this work possess a very fine morphology with less distinct phase separation and an inorganic phase finely dispersed through the organic matrix than in other organic–inorganic sol–gel systems. Once again, high PSA molecular weights and more branched materials showed a higher degree of scattering due to greater immiscibility.

Generally, it appeared that the TEM graphs produced for this work did not clearly show any texture due to the presence of domains in the matrix. The lack of features in the TEM images is thought to be due to the very fine nature of the dispersion in our materials, as in other more highly scattering sol–gel organic–inorganic systems the inorganic phase can be seen by TEM [39,40]. It can thus be concluded that most of the samples have a microstructure in the low nanometer range, with the inorganic phase finely dispersed throughout the organic matrix. Combined with the results from fractal analysis of the SAX data, it appears that the silicate domains formed in this work are particularly wispy and fine, compared with other more developed phase-separated sol–gels previously reported [39,40].

It was determined that the densities varied from sample to sample but were always close to that of PHEMA which dominates the total composition. An inverse relationship between PALS free volume size and increased acid concentration (greater branched PSA inclusions) leads to the idea of increasingly immiscible systems possibly having additional free volume at the interface. However, an opposite (although less clear) trend was observed for materials made at particular acid concentration and differing PSA polymerization time. It seemed that more highly branched, separated morphologies led to a slight decrease in free volume size and concentration which was suggested to be related to the effect of such fine phase-separated structures on molecular constraint of the organic phase surrounding the particles. The changes in packing in the system observed in PALS were not, however, clearly reflected in variation of bulk densities. However, it should be noted that PALS detects angstrom-sized free volume whereas bulk density may be related to larger scale packing and ordering. The PALS results did seem to indicate that despite the low concentration of silicate phase the very fine scale of its dispersion does lead to strong amount of interactions with the organic phase which influences its molecular packing.

Acknowledgements

Financial support from the Australian Government and SOLA International Holdings Ltd was gratefully appreciated.

References

[1] Wilkes GL, Orler B, Huang H. Polym Prepr 1985;26:300.
[2] Novak BM, Grubbs RH. J Am Chem Soc 1988;110:7542.
[3] Schmidt H, Krug H. ACS Symp Ser 1994;572:183.

[4] Pope EJA. Chemical processing of ceramics. New York: Marcel Dekker, 1994 p. 265.
[5] Mascia L. TRIP 1995;3(2):61.
[6] Hu Y, Mackenzie JD. J Mater Sci 1992;27:4415.
[7] Wen J, Wilkes GL. Chem Mater 1996;8:1667.
[8] Mackenzie JD, Huang Q, Iwamoto T. J Sol–Gel Sci Technol 1996; 7:151.
[9] Huang H, Wilkes GL, Carlson JG. Polymer 1989;30:2001.
[10] Wang B, Wilkes GL, Hedrick JC, Liptak BC, McGrath JE. Macromolecules 1991;24:3449.
[11] Noel JLW, Wilkes GL, Hedrick JC, Liptak BC, McGrath JE. J Appl Polym Sci 1990;40:1177.
[12] Nass R, Arpac E, Glaubitt W, Schmidt H. J Non-Cryst Solids 1990; 121:370.
[13] Schmidt H, Kasemann R, Burkhart T, Wagner G, Arpac E, Geiter E. Hybrid organic–inorganic composites. Washington: ACS, 1995 p. 331.
[14] Wei Y, Bakthavatchalam R, Whitecar CK. Chem Mater 1990;2:337.
[15] Wojcik AB, Klein LC. J Sol–Gel Sci Technol 1995;4:57.
[16] Fitzgerald JJ, Landry CJT, Pochan JM. Macromolecules 1992; 25:3715.
[17] Klein LC, Abramoff B. Polym Prepr 1991;32(3):519.
[18] Landry CJT, Coltrain BK, Landry RM, Fitzgerald JJ, Long VK. Macromolecules 1993;26(14):3702.
[19] Grey CP, Sharp KG. Mater Res Soc Symp Proc 1996;435:179.
[20] Yin W, Li J, Wu J, Gu T. J Appl Polym Sci 1997;64(5):903.
[21] Yoshida M, Prasad PN. Chem Mater 1996;8:235.
[22] Habsuda J, Simon GP, Hewitt DG, Cheng Y-B, Toh H. Proceedings of Organic–Inorganic Hybrids Conference. Guildford University of Surrey, 2000.
[23] Simon GP. Trends Polym Sci 1997;5(12):394.
[24] Jean YC. Microchem J 1990;42:72.
[25] Mogensen OE. Positron annihilation in chemistry. Amsterdam: Springer, 1995.
[26] Pethrick RA. Prog Polym Sci 1997;22(1):1.
[27] De Sousa EMB, De Magalhaes WF, Mohallem NDS. J Phys Chem Solids 1999;60(2):211.
[28] Misheva M, Djourelov N, Margaca FMA, Salvado IMM. J Non-Cryst Solids 2000;272(2-3):209.
[29] Wakabayshi Y, Li HL, Ujihira Y, Kamitani K, Inoue H, Makishima A. Mater Sci Forum 1997;255-257:357.
[30] McCrum NG, Read B, Williams G. Anelastic and dielectrics effects in polymeric solids. New York: Wiley, 1967.
[31] Fried JR, Karasz FE, MacKnight WJ. Macromolecules 1978;11(1): 150.
[32] Roland CM, Ngai KL. Macromolecules 1991;24:2261.
[33] Spall S, Goodwin AA, Zipper MD, Simon GP. J Polym Sci, Part B: Polym Phys 1996;34:2419.
[34] Yamada N, Yoshinaga I, Katayama S. J Mater Chem 1997;7(8):1491.
[35] Schartel B, Wendorff JH. Polymer 1995;36(5):899.
[36] Ngai KL, Schönhals A. J Polym Sci, Part B: Polym Phys 1998; 36:1927.
[37] Schmidt PW. Modern aspects of small-angle scattering. Dordrecht: Kluwer, 1995.
[38] Schaefer DW, Keefer KD. Better ceramics through chemistry. New York: North-Holland, 1984 p. 1.
[39] Bauer BJ, Liu DW, Jackson CL, Barnes JD. Polym Adv Technol 1996;7:333.
[40] Jackson CL, Bauer BJ, Nakatani AI, Barnes JD. Chem Mater 1996;8:727.
[41] David IA, Scherer GW. Chem Mater 1995;7:1957.
[42] Landry CJT, Coltrain BK, Brady BK. Polymer 1992;33(7):1486.
[43] Haraguchi K, Usami Y, Ono Y. J Mater Sci 1998;33(13):3337.
[44] Campbell JA, Goodwin AA, Ardi MS, Simon GP. Macromol Symp 1997;118:383.
[45] Jean YC, Deng Q. J Polym Sci, Part B: Polym Phys 1992;30:1359.